


DOI 10.24425/aee.2023.145411

# Practical aspects of testing superconducting electromagnets by the capacitor discharge method taking into account the non-linearity of circuit parameters

MICHAŁ MICHNA<sup>1</sup>  , ANDRZEJ WILK<sup>1</sup> , MAREK WOŁOSZYK<sup>1</sup> , MICHAŁ ZIÓŁKO<sup>1</sup> ,  
STANISŁAW GALLA<sup>1</sup> , PIOTR SZWANGRUBER<sup>2</sup> 

<sup>1</sup>*Gdansk University of Technology, Faculty of Electrical and Control Engineering  
Gabriela Narutowicza str. 11/12, 80-233 Gdańsk, Poland*

<sup>2</sup>*GSI Helmholtzzentrum für Schwerionenforschung GmbH  
Darmstadt 64291, Germany*

*e-mail: {  [@pg.edu.pl](mailto:michal.michna/andrzej.wilk/marek.woloszyk/michal.ziolko/stanislaw.galla),  
[p.szwangruber@gsi.de](mailto:p.szwangruber@gsi.de) }*

(Received: 15.06.2022, revised: 03.11.2022)

**Abstract:** The article presents selected issues related to the development and testing of the diagnostics systems dedicated for superconducting electromagnets. The systems were constructed to assess the production quality of superconducting electromagnets of the SIS100 synchrotron, a new accelerator being built as part of the Facility of Antiproton and Ion Research (FAIR). One of the systems is used for automatic checking of electrical connection parameters and the continuity of electric circuits. The role of the second device is to assess the quality of winding insulation and to estimate circuit parameters of electromagnet coils using the capacitor discharge method. The work presents measurements and analysis of current and voltage waveforms acquired during discharges on a magnet coil simulator and on the SIS100 main dipole electromagnet.

**Key words:** diagnostic, discharge method, superconducting electromagnets

## 1. Introduction

The Facility for Antiproton and Ion Research (FAIR) which is currently under construction in Darmstadt, Germany, will be one of the largest research laboratories in the world available to the physics community [1]. One of the most important machines of FAIR will be the superconducting



© 2023. The Author(s). This is an open-access article distributed under the terms of the Creative Commons Attribution-NonCommercial-NoDerivatives License (CC BY-NC-ND 4.0, <https://creativecommons.org/licenses/by-nc-nd/4.0/>), which permits use, distribution, and reproduction in any medium, provided that the Article is properly cited, the use is non-commercial, and no modifications or adaptations are made.

(SC) SIS100 synchrotron of which the main magnetic lattice is constructed from fast-cycling SC dipole and quadrupole electromagnets [2] (Fig. 1). SIS100 superconducting electromagnets are of the super-ferric window-frame type, with coils made of Nb-Ti Nuclotron-type cable [3–5]. Their magnetic yokes are made of a 1 mm thick steel sheet [2, 6–8].

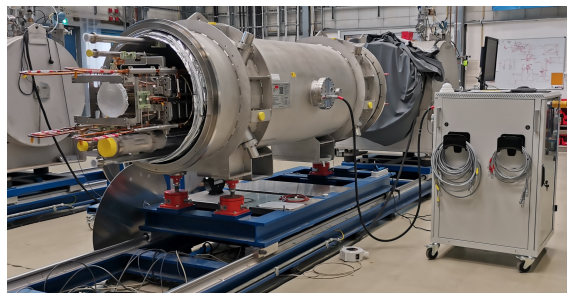


Fig. 1. Superconducting SIS100 dipole magnet at the test bench in GSI Darmstadt, Germany

SC magnets are complicated and expensive devices; therefore, an important issue is the assessment of production quality and technical conditions during maintenance shutdowns of the machine. The assessment of the quality of insulation and continuity of the main winding circuits and sensor circuits are important SC diagnostic tests. The team from the Faculty of Electrical and Control Engineering of the Gdansk University of Technology (GUT) has developed two measurement systems dedicated to SC magnet diagnostic [9–12]. The first device is designed to perform an automatic check of the connection correctness and continuity of electric circuits. The task of the second device is to assess the quality of winding insulation using the capacitor discharge method as well as to estimate circuit parameters of SC electromagnet coils. It is assumed that an inter-turn coil insulation fault affects the resultant value of resistance and inductance. The measurement of insulation resistance between the SC electromagnet coil and its housing is conducted at applied high dc voltage (3 kV). This paper focuses on the practical aspects of the development and testing of the capacitor discharge diagnostic system (CDDS).

The SC cable (Nuclotron-type) used for the coils of the main SIS100 magnets has a complex mechanical structure [13–15]. In the middle of the cable (Fig. 2), there is a CuNi cooling tube, surrounded by a layer of superconducting transposed strands. The strands are attached by NiCr wire and insulated with polyimide tape (Kapton) [4]. The SC electromagnet operates at temperature 4 K. Table 1 shows the parameters of the SIS100 dipole electromagnet.

The estimation of the SC winding circuit parameters (resistance and inductance) in the dissipative state requires high electrical current density. However, the test time should be limited in order to not damage the conductor. The developed diagnostic system uses the capacitor discharge method. It is a non-destructive diagnostic method commonly used to find turn-to-turn insulation failures in electrical machines [16, 17]. In this method, the transient current and voltage waveforms observed during the discharge of the capacitor connected to the tested winding, are recorded and analyzed. An important issue is the influence of the internal circuit parameters of the diagnostic system (such as the capacitor bank, electronic switch based on insulated gate bipolar transistor (IGBT), and connection cables) on the analyzed waveforms. Additionally, based on the tests

Table 1. SIS100 dipole magnet parameters [14]

Parameter	
Max air-gap field, T	1.9
Effective magnetic length, m	3.062
Layers $\times$ turns	1 $\times$ 8
Operating current, kA	13.2
Critical current @ 2.1 T, 4.7 K, kA	19.84
Outer diameter of cooling tube, mm	5.7
Number of strands	23
Strand diameter, mm	0.8
Cable cross-section, mm <sup>2</sup>	6.09

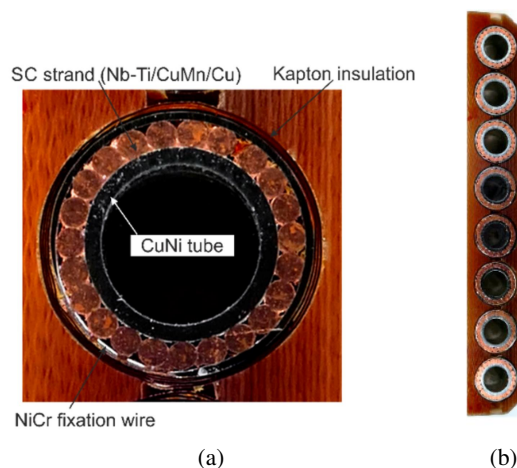


Fig. 2. NbTi Nuclotron-type cable of SIS100 superconducting electromagnet (a), cross-section of the main dipole coil (b)

performed, it was shown that non-linear resistance of the IGBT switch has a significant impact on the discharge currents waveforms. Correct estimation of the circuit parameters of the SC electromagnet coil requires the determination of the internal impedance characteristics of the diagnostic system and the assessment of their impact on the accuracy of the measurement.

The novel aspects of this work include:

- Presentation of the original and unique programmable diagnostic system with adjustable properties: capacity up to 3.2  $\mu\text{F}$ , voltage up to 3 kV, programmable sequence of voltages and discharge capacities.

- Determination of the nonlinear circuit parameters of the special emulator device for testing and calibration of capacity discharge diagnostic system.
- Determination of the internal nonlinear circuit parameters of the capacitor discharge system as a function of maximum discharge current and for different discharge capacitances.
- Determination of the internal resistance of the IGBT switch as a function of discharge current.
- Proposing methodology for waveform parameters analysis to determine superconducting winding parameters taking into account the non-linearity circuit parameters of capacity discharge diagnostic system.

This paper aims to achieve the following objectives:

- Description of the programmable diagnostic system with adjustable properties and diagnostic method for estimation of superconducting magnet parameters.
- Description of the special emulator device for testing and calibration of capacity discharge diagnostic system.
- Estimating the non-linear circuit parameters of the capacity discharge system and emulator testing device.
- Development of the methodology for waveform parameters analysis to determine superconducting winding parameters.

## 2. Capacitor discharge diagnostic method

The quality of winding insulation will be checked based on the capacitor discharge test result [16–18]. The discharge test is a non-destructive diagnostic method in which the insulation condition and circuit parameters are evaluated by an analysis of voltage and current waveforms acquired during discharge of capacitance bank on the coil under test (Fig. 3).

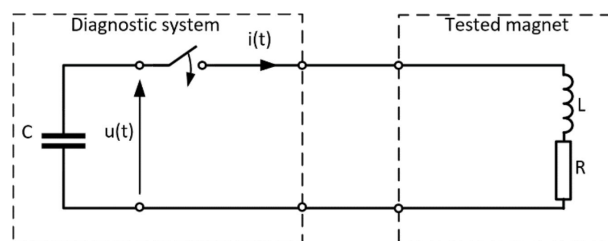


Fig. 3. Simplified diagram of the capacitor discharge diagnostic system

The capacitor discharge test is performed on a device disconnected from its powering system. The diagnostic method uses a transient state for winding insulation fault detection. The capacitor bank, charged to a predefined voltage, is being discharged on the coil. During the test, the current and the coil voltage are recorded simultaneously.

The following criteria can be used to assess the quality of insulation:

- Waveform parameters analysis – this method is based on calculating and comparing waveform parameters like frequency and damping factor. The reference value of the parameters should be provided to the system or calculated from winding design data (Table 2),

- Waveform comparison method – measured discharge waveform is compared with a reference waveform and the quality factor is calculated based on the least mean square error (LMSE) or error area ratio (EAR) [19].

## 2.1. Waveform parameters analysis

The waveforms' shapes depend on the measurement circuit parameters: capacitance of the capacitor bank ( $C$ ), resistance ( $R$ ) and inductance ( $L$ ) of the tested coil. The insulation quality is often assessed by comparing the measured frequency with the reference frequency. The effectiveness of this method depends mainly on the number of shorted turns and the short-circuiting impedance.

The measured current and voltage waveforms of the capacitor discharge through the SC windings, can be simplified as:

$$i(t) = I_m e^{-\beta t} \sin(\omega \cdot t), \quad (1)$$

$$u(t) = U_c e^{-\beta t} \left( \cos(\omega \cdot t) + \frac{\beta}{\omega} \sin(\omega \cdot t) \right), \quad (2)$$

where:  $I_m, U_c$  represent the current and voltage amplitude,  $\beta = R/2L$  is the damping,  $\omega_0 = 1/\sqrt{LC}$  is the resonance frequency and natural frequency:

$$\omega = 2\pi f = \sqrt{\omega_0^2 - \beta^2} = \sqrt{\frac{1}{LC} - \left(\frac{R}{2L}\right)^2}. \quad (3)$$

The waveform parameters can be estimated based on the analysis of the measurement waveforms. The natural frequency of the oscillation signal is calculated based on the period determined as the time between adjacent zero crossings of the signal. The damping factor is determined as:

$$\beta = \Lambda f, \quad (4)$$

where  $\Lambda$  is the logarithmic decrement of damping; determined from the ratio of subsequent amplitudes ( $A_n$ ) of the measured signal:

$$\Lambda = \frac{1}{m-n} \ln \left( \frac{A_n}{A_m} \right), \quad (5)$$

where  $A_n$  and  $A_m$  denote the  $n$ -th and  $m$ -th discharge waveform peak or valley, respectively. The waveforms parameters can be also determined using the nonlinear curve fitting method (Levenberg–Marquardt) [20, 21]. In this method, the waveform equation, measurements points and initial parameters are defined as an input. The best-fit parameters are calculated to minimize the weighted mean square error between the measurement waveforms and the best nonlinear fit.

Based on the waveform parameters ( $\beta, \omega$ ), the parameters of the equivalent circuit of the tested magnet winding can be calculated as:

$$\begin{aligned} L &= \frac{U_m}{\omega I_m}, \\ R &= 2\beta L = 2 \frac{U_m \beta}{I_m \omega}. \end{aligned} \quad (6)$$

The choice of reliable and effective acceptance criteria is an important step in the development of the diagnostic system. Typically, frequency and damping factor ( $\beta$ ) analysis are used for the comparison and evaluation of the V-I waveforms. In the case of SC electromagnets of SIS100, the discharge circuit is characterized by a high dynamic resistance due to induced AC losses in the yoke. Therefore  $\beta$  is high and frequency-dependent. The V-I waveforms vanish after a few oscillations. The application of various analysis methods based on FFT is limited due to the high  $\beta$  which distorts the frequency spectrum.

## 2.2. Waveform comparison method

The waveform comparison method consists in comparing the measured current or voltage waveforms with the reference waveforms for the tested winding. To evaluate the differences between the two waveforms, the quality factor is calculated based on the least mean square error (LMSE) or error area ratio (EAR).

The LMSE factor is calculated based on the least mean square method:

$$\text{LMSE} = \left( \frac{1}{N} \sum_{i=1}^N \left( W_i^{(\text{ref})} - W_i^{(\text{test})} \right)^2 \right)^{\frac{1}{2}}, \quad (7)$$

where:  $W_i^{(\text{ref})}$  is the  $i$ -th point of the reference waveform,  $W_i^{(\text{test})}$  is the corresponding point of the test waveform,  $N$  is the number of data points that are compared. The reference waveform is generated on the basis of the model described by Eq. (1) or (2) and the rated values of resistance and inductance of the tested winding.

The EAR factor is calculated based on the equation:

$$\text{EAR} = \frac{\sum_{i=1}^N \left| W_i^{(\text{ref})} - W_i^{(\text{test})} \right|}{\sum_{i=1}^N \left| W_i^{(\text{ref})} \right|}. \quad (8)$$

Two identical waveforms just have the zero value of the LMSE and EAR factors. If the value of the factors changes by more than the value expected (threshold), this is an indicator of poor insulation quality or detection of short-circuits in windings of a tested magnet.

## 3. Diagnostic system

The diagnostic system for SIS100 SC magnets insulation quality testing developed at the GUT consists of two devices: the main capacitor discharge diagnostic system placed in a mobile rack stand and the SC winding simulator (SCWS) placed in the suitcase (Fig. 5).

### 3.1. Capacitor discharge diagnostic system

The block diagram of the capacitor discharge diagnostic system (CDDS) is shown in Fig. 4 and the CDDS unit is shown in Fig. 5. The main task of the device is to perform a discharge test. The measurement sequence consists of the following steps: charging the main capacitor, calibrating the capacitance, applying a voltage to the winding under test via the IGBT power

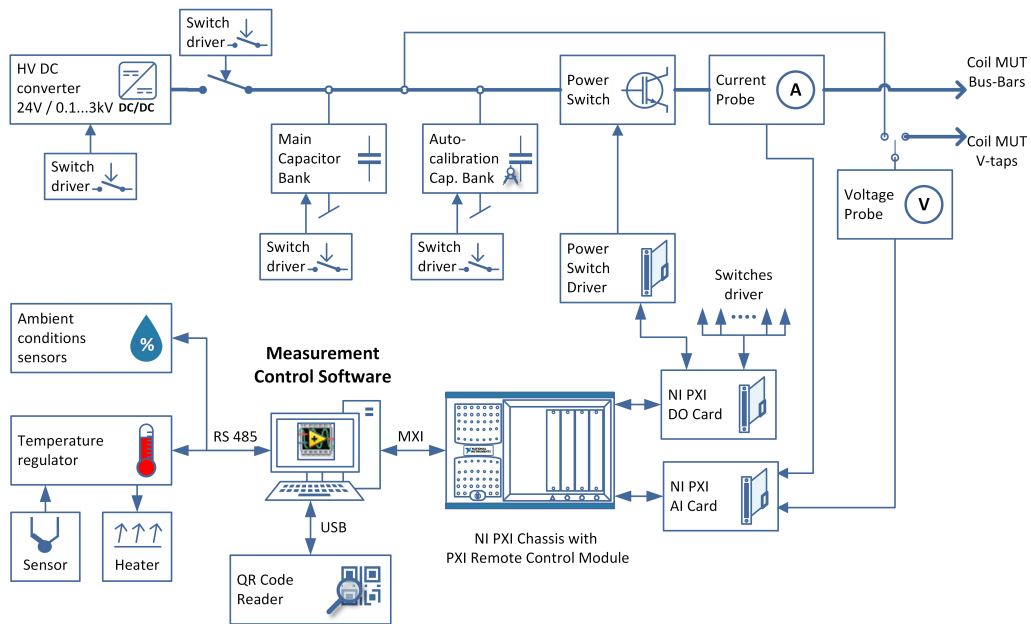


Fig. 4. The general structure of the capacitor discharge diagnostic system connected to the magnet under test (MUT)

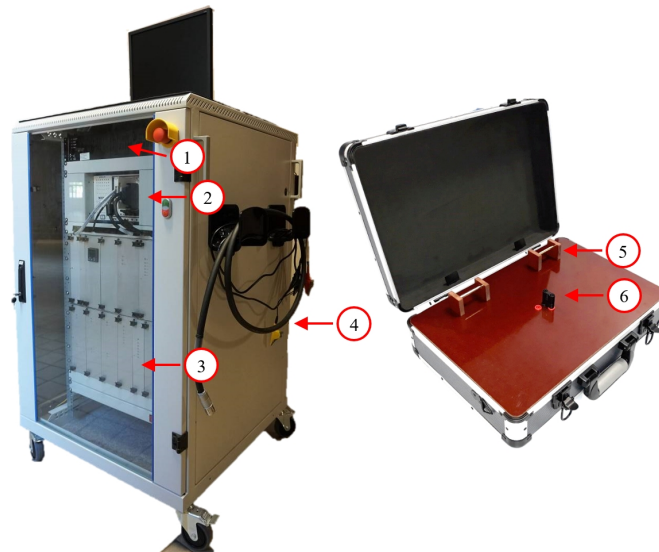


Fig. 5. Front-right view of the capacitor discharge diagnostic system unit (left) and SC winding simulator (right): 1 – control computer, 2 – NI PXI chassis with NI PXI remote control module, NI PXI DAQ card and NI PXI DIO card, 3 – main capacitor bank, 4 – test leads, 5 – HV test leads connection points, 6 – banana jumper for CDS configuration

switch, and measuring the current and voltage waveforms. The CDDS is equipped with systems for controlling ambient conditions (internal and external temperatures and humidity). Control and measurement functions of the diagnostic system were implemented using a set of National Instruments [21] devices and the measurement control software was developed in LabVIEW graphical programming environment [22].

### 3.2. SC winding simulator

SC winding simulator (SCWS) is the special device for emulating the inductance and resistances of SIS100 dipole electromagnet windings both in undamaged and damaged conditions (Fig. 5). The core element of the SCWS is a double-layer air coil, with a lead-out in 1/4 of the winding's length. The SCWS enables emulating of two faults: an inter-turn short-circuit and a short-circuit after overvoltage of 1 kV. A banana jumper is used to change the emulator configuration. The outer dimensions of the suitcase are 31 cm long, 45 cm wide and 15 cm high. The total weight of the SCWS is approximately 8 kg.

## 4. Measurement results

The CDDS was designed to test the quality of winding insulation of various types of SC magnets used in the construction of the SIS100 synchrotron. Considering circuit parameters of these coils, it was found that the range of expected frequencies of discharge waveforms is from 300 Hz to 8 kHz and the expected maximum value of the discharge current from a few amperes up to 215 A (Table 2). Therefore, it is important to analyze the CDDS parameters as a function of the frequency and discharge current.

Table 2. Reference parameters of the tested SC coils

Coil types	$U$ [V]	$C$ [ $\mu$ F]	$R$ [ $\Omega$ ]	$L$ [mH]	$f$ [Hz]	$I_{\max}$ [A]
corrector CS	1 100	1.0	63	47	726.3	5.1
corrector MO	1 100	1.0	60	7.4	1 734.0	13.6
corrector MQ	1 100	1.0	40	1.1	3 828.0	41.6
corrector MS	1 100	1.0	50	5.6	2 004.6	15.6
corrector QJ	1 000	2.0	0.021	0.33	6 195.1	77.8
corrector SH	1 100	1.0	70	28	930.1	6.7
corrector SV	1 100	1.0	70	28	930.1	6.7
main DP	3 000	2.0	0.235	0.55	4 798.6	180.9
main F1	3 000	2.0	0.235	0.55	4 798.6	180.9
main F2	3 000	2.0	0.132	0.39	5 698.6	214.8
main LQ(X)	1 100	2.0	70	140	298.1	4.2
main LQ(Y)	1 100	2.0	70	140	298.1	4.2
main QD	3 000	2.0	0.132	0.39	5 698.6	214.8
DP symulator	1 100	2.0	0.304	0.206	7 840.0	108.4



#### 4.1. SCWS ant test leads impedance

The Keysight E4990A impedance analyzer was used to measure the impedances of the SCWS and test leads. Based on the measurements, the resistance and inductance characteristics were determined as a function of frequency (Fig. 6, Fig. 7). The simulator was made as a coil

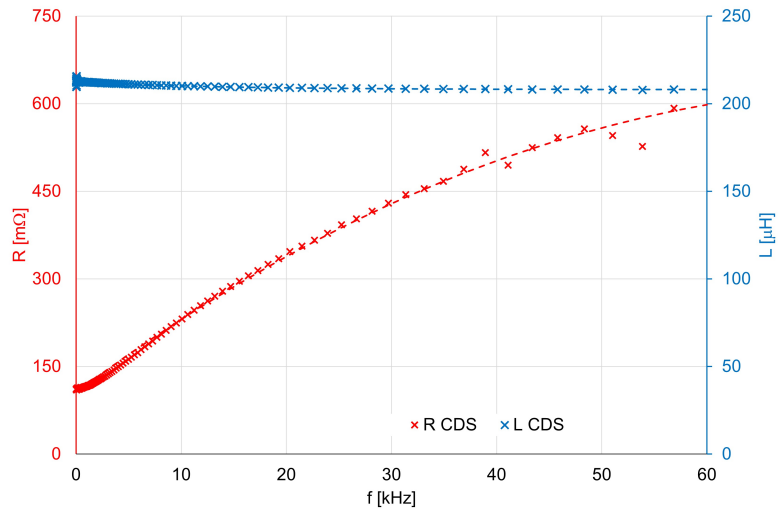


Fig. 6. Resistance (red) and inductance (blue) of the SCWS winding as a function of frequency: crosses mark the measuring points, the dashed line indicates a fitting function described by Eq. (9)

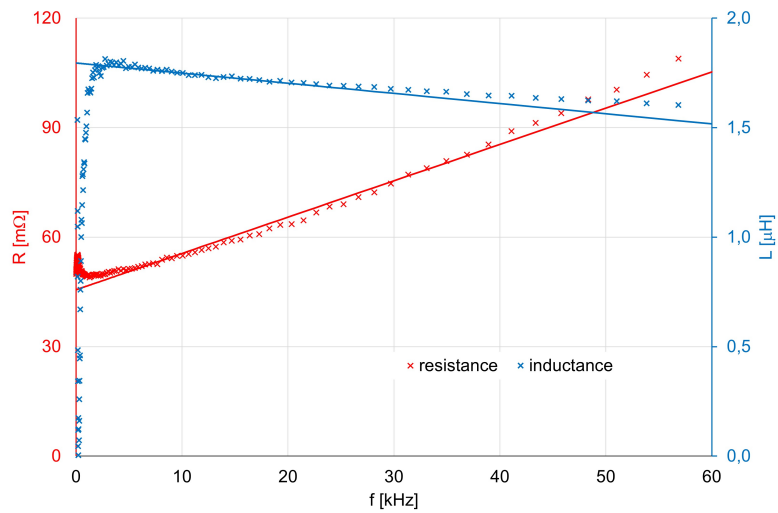


Fig. 7. Resistance (red) and inductance (blue) of the series-connected kelvin crocodile clips, the test lead and the socket as a function of frequency: crosses mark the measuring points, the solid line indicates a fitting function described by Eq. (10)

without a ferromagnetic core, therefore the inductance is constant in a wide range of frequencies ( $L_{SCWS} = 210 \mu\text{H}$ ). The increase in the SCWS resistance is influenced by the skin effect, which reduces the active cross-section of the coil wires. The change in SCWS resistance and inductance as a function of frequency can be approximated by:

$$\begin{aligned} R_{SCWS}(f) &= 106.0 + 13.3 \cdot 10^{-3} f - 85.0 \cdot 10^{-9} f^2 \text{ [m}\Omega\text{]}, & R^2 &= 99.6\%, \\ L_{SCWS}(f) &= 208.04 + 4.5 \cdot e^{-75.2 \cdot 10^{-6} f} \text{ [\mu H]}, & R^2 &= 99.8\%. \end{aligned} \quad (9)$$

The test lead impedance includes the leads themselves that are connected in series with the kelvin crocodile clips and the socket. The measurement results are shown in Fig. 7. The increase in resistance at higher frequencies is due to the skin effect. Their resistance and inductance as a function of frequency can be calculated using the following equations:

$$\begin{aligned} R_{leads}(f) &= 45.6 + 1.0 \cdot 10^{-3} f \text{ [m}\Omega\text{]}, & R^2 &= 98.8\%, \\ L_{leads}(f) &= 1.8 \cdot 10^{-6} - 3.94 \cdot 10^{-12} f \text{ [\mu H]}, & R^2 &= 90.2\%. \end{aligned} \quad (10)$$

#### 4.2. CDDS impedance

The CDDS impedance covers all components of the device, from the main capacitor bank, through the power IGBT switch, internal connections, up to the test leads. Measurement of the CDDS impedance allows determine correction functions in order to correctly calculate circuit parameters of tested SC magnet coils.

To determine the CDDS parameters, a series of discharge tests with the use of SCWS were performed for two capacitances ( $1.5 \mu\text{F}$  and  $2 \mu\text{F}$ ) and voltages of the capacitor bank. Figure 8 shows the discharge current waveforms for the  $2 \mu\text{F}$  bank capacity and different voltage levels.

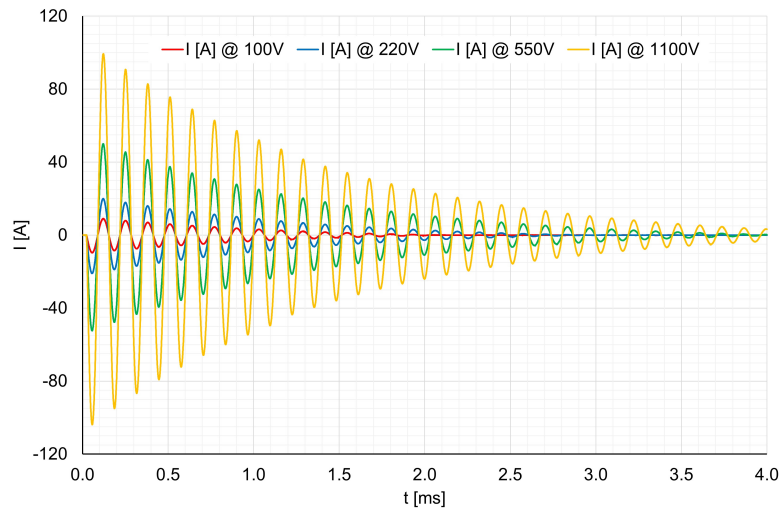


Fig. 8. Discharge current waveforms for different voltage levels and capacitance  $C = 2 \mu\text{F}$  recorded in tests using CDDS and SCWS

The discharge current waveforms were the basis for the estimation of tested circuit parameters using the Levenberg–Marquardt non-linear curve fitting method (Fig. 9). The capacity values are correctly identified and amount to 1.5  $\mu\text{F}$  and 1.98  $\mu\text{F}$ . The expected values of the SCWS inductance for both capacities should be 210.3  $\mu\text{H}$  and 211  $\mu\text{H}$ , and the mean of the estimated inductance was 213  $\mu\text{H}$  and 215  $\mu\text{H}$ , respectively. A large difference between the estimated and the expected value was noted in the case of SCWS resistance. The expected resistance should be 218  $\text{m}\Omega$  and 203  $\text{m}\Omega$ , but based on CDDS measurements, average resistance of 390  $\text{m}\Omega$  and 372  $\text{m}\Omega$  were obtained. Additionally, a large dispersion of the resistance values identified at different values of the discharge voltage can be observed (Fig. 9). This means that frequency is not the only factor affecting the internal impedance of the CDDS.

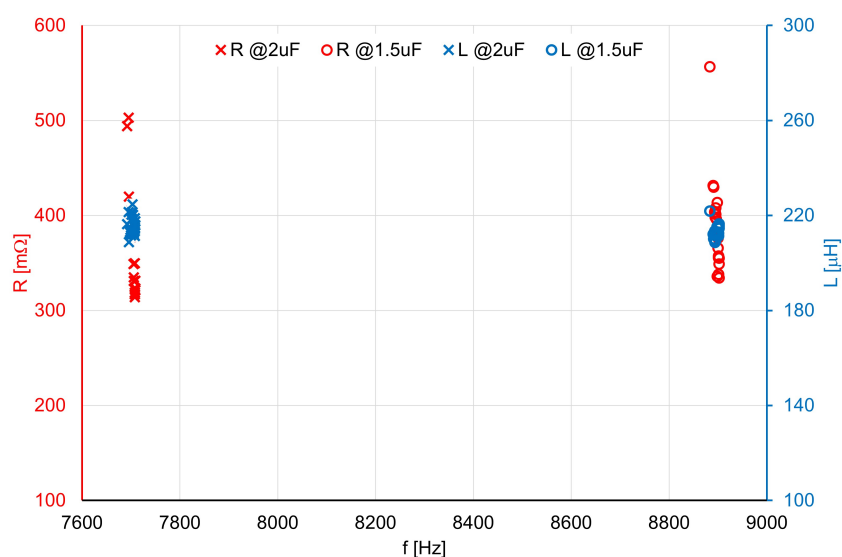


Fig. 9. Parameters of the SCWS estimated by CDDS as a function of frequency: resistance (red) and inductance (blue)

Figure 10 shows the CDDS impedance as a function of the maximum value of the discharge current. The changes in the CDDS inductance are small, of the order of about 4  $\mu\text{H}$ .

A significant nonlinearity is observed for the CDDS resistance (Fig. 11). The CDDS resistance is the sum of the capacitor series resistance (equivalent series resistance ESR), the IGBT power switch resistance, the resistance of the internal connections and the socket, the resistance of the test lead and kelvin crocodile clips.

The capacitor bank was made using a metallized polypropylene film capacitor with low self-inductance and low ESR. The non-linearity of the CDDS resistance is mainly due to the non-linearity of the  $I_c$ - $V_{ce}$  characteristic of the IGBT switch (Fig. 12). The internal resistance of the IGBT switch was calculated as the ratio of the collector-emitter voltage to the collector current.

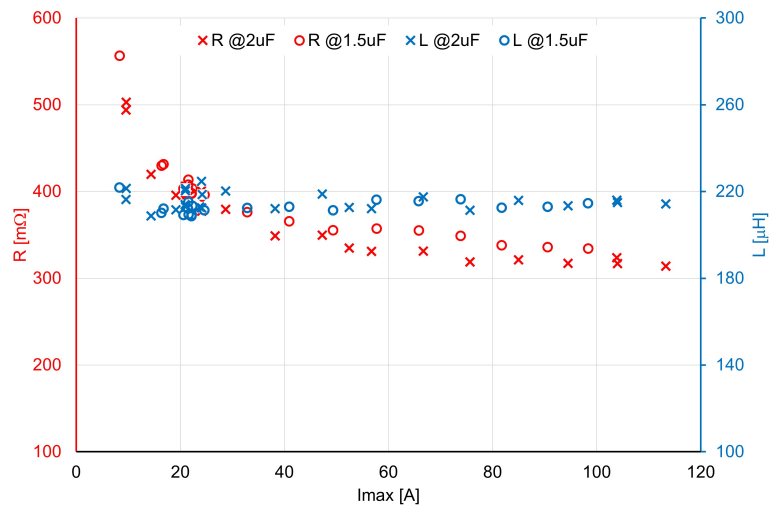


Fig. 10. Estimated parameters of the SCWS as a function of discharge maximum current and for different discharge capacitances: resistance (red) and inductance (blue)

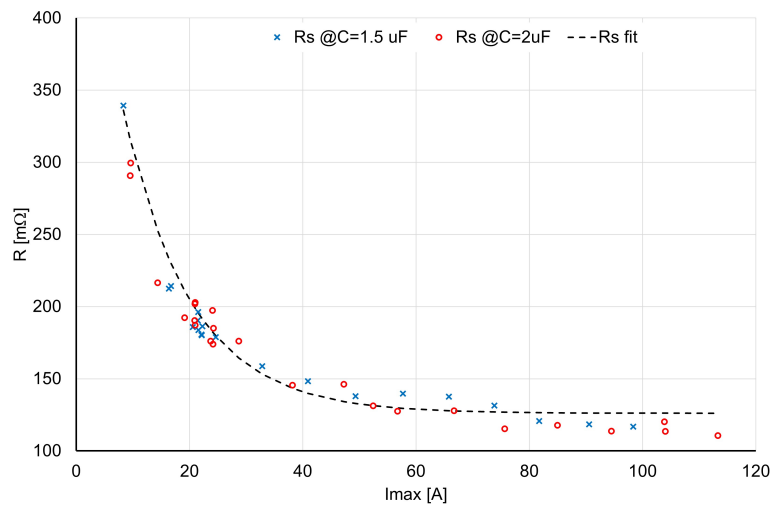


Fig. 11. Resistance of the CDSS as a function of maximum discharge current, determined from measurements for different capacitance values

The shape of the resistance characteristic as a function of the collector current (Fig. 13) corresponds to the non-linearity of the CDSS resistance (Fig. 11). This supports the finding that the main cause of CDSS impedance nonlinearity is the nonlinear conduction characteristic of the IGBT switch.

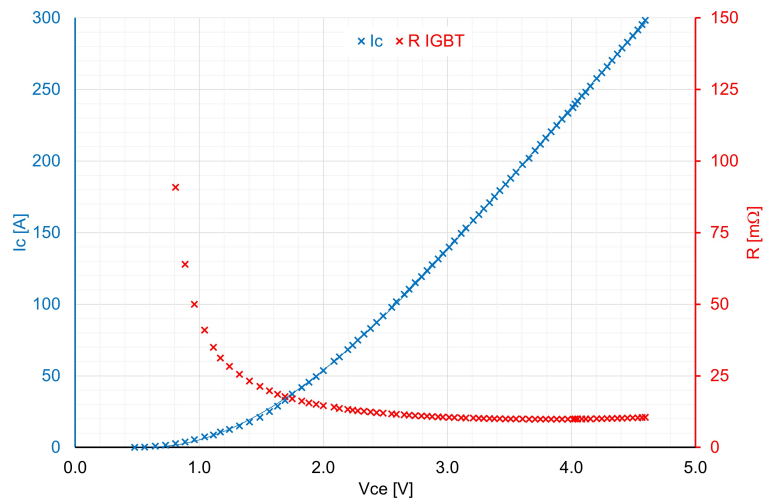


Fig. 12. The characteristics of the IGBT switch: collector current versus collector-emitter voltage in blue, and IGBT internal resistance versus collector-emitter voltage in red

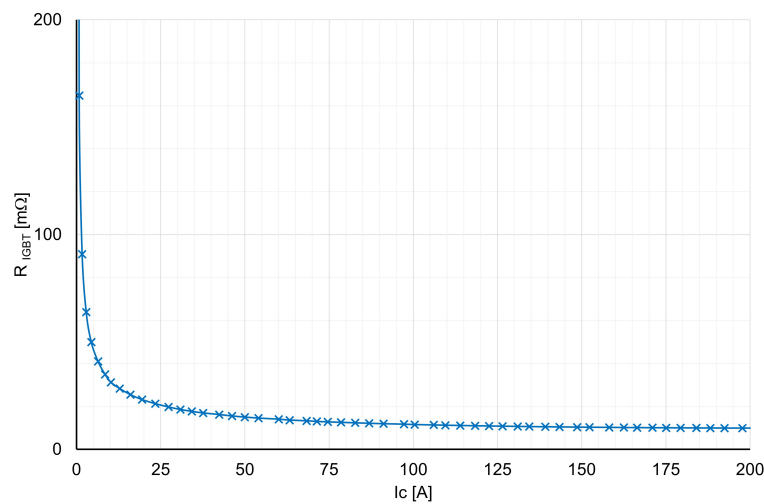


Fig. 13. The internal resistance of the IGBT switch as a function of collector current

To calculate the correct values of the parameters of the tested electrical circuit, it is necessary to apply the correction considering the internal impedance of the CDDS:

$$\begin{aligned}
 R_{\text{CDDS}}(I_{\text{max}}) &= 126 + 420e^{-0.08} I_{\text{max}} \text{ [m}\Omega\text{]}, \\
 L_{\text{CDDS}}(f) &= 4 \text{ [\mu H]}.
 \end{aligned}
 \tag{11}$$

### 4.3. Discharge test on SIS100 dipole SC magnets

The developed procedure for carrying out the discharge test, considering the correction resulting from the internal impedance of the CDDS, was tested with the use of SCWS (Fig. 1). The parameters of the SCWS electrical circuit are correctly estimated by the fitting procedure. The quality factors LMSE and EAR indicate the difference between the reference and the measured waveform.

The CDDS has also been checked for proper operation when connected to the windings of the SIS100 dipole SC electromagnets at the test bench in GSI Darmstadt, Germany [23] (Fig. 1). Tests were performed without connection to the cryostat at ambient temperature. The tests aimed to check the correct operation of the diagnostic device and to determine the electrical circuit parameters of the SC magnet winding. The measurement results at the voltage of 3 kV and capacitance of 1 uF are shown in Fig. 14.

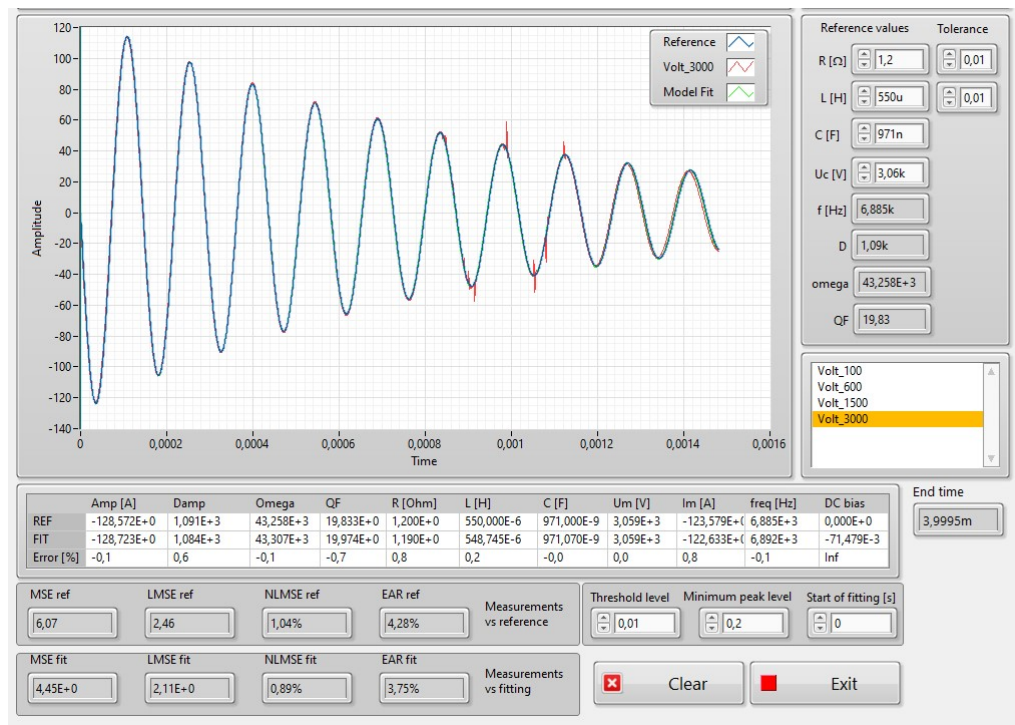


Fig. 14. Discharge test results on SIS100 dipole SC magnet at 3 kV and 1 uF bank capacity

## 5. Conclusions

The Nuclotron-type cable, from which an SC magnet is coiled, has a relatively complex electrical and mechanical structure. The electromagnet windings are tested in order to assess the quality of the insulation condition and to determine the electrical circuit parameters. For this

purpose, a prototype of a diagnostic system based on the measurement and analysis of current and voltage waveforms in the transient state caused by a capacitor discharge was developed. In this transient state, all important nonlinearities of the electrical discharge circuit should be taken into account to determine the most accurate coil parameter values. Based on the measurements and analysis carried out, the authors present the following conclusions:

- Prototype of the original and unique programmable diagnostic system with adjustable properties: capacity up to 3.2  $\mu\text{F}$ , voltage up to 3 kV are sufficient to create transient states for the determination of the electrical parameters of SIS100 synchrotron electromagnet windings without a chamber tube.
- For calibration purposes of the diagnostic system prototype, the determination of the non-linear circuit parameters of the special emulator device and connecting cables is necessary. Resistance values show great dependence as a function of the frequency.
- Internal circuit parameters of the presented prototype of the diagnostic system were analyzed as a function of frequency and maximum discharge current. The exponential dependence of the internal resultant resistance value as a function of the maximum current value was determined – Eq. (11).
- The resistance of the IGBT switch is a key component of the internal resultant resistance. Strong resistance non-linearity is observed in the range of currents from 0 to several dozen Amperes.
- A methodology for the analysis of measured waveforms to determine superconducting winding parameters considering non-linearity circuit parameters of the capacity discharge diagnostic system, using the Levenberg–Marquardt non-linear curve fitting method, is proposed.

## References

- [1] Facility for Antiproton and Ion Research in Europe GmbH (FAIR GmbH), <https://fair-center.eu/>, accessed January 2022.
- [2] Mierau A. *et al.*, *Testing of Series Superconducting Dipole Magnets for the SIS100 Synchrotron*, IEEE Transactions on Applied Superconductivity, vol. 29, no. 5, pp. 1–7 (2019), DOI: [10.1109/TASC.2019.2904693](https://doi.org/10.1109/TASC.2019.2904693).
- [3] Khodzhbagiyani H. *et al.*, *Design of new hollow superconducting NbTi cables for fast cycling synchrotron magnets*, IEEE Transactions on Applied Superconductivity, vol. 13, no. 2, pp. 3370–3373 (2003), DOI: [10.1109/TASC.2003.812323](https://doi.org/10.1109/TASC.2003.812323).
- [4] Khodzhbagiyani H.G., Kovalenko A.D., Fischer E., *Some aspects of cable design for fast cycling superconducting synchrotron magnets*, IEEE Transactions on Applied Superconductivity, vol. 14, no. 2, pp. 1031–1034 (2004), DOI: [10.1109/TASC.2004.830386](https://doi.org/10.1109/TASC.2004.830386).
- [5] Chorowski M., Cholewiński M., Tomków Ł., Cizek M., *Numerical assessment of thermal behaviour of a superconducting bus-bar with a Nuclotron-type cable*, Archives of Electrical Engineering, vol. 69, no. 2, pp. 365–377 (2020).
- [6] Velasco J.C. *et al.*, *Design of the Superconducting Extraction and Injection Quadrupole Doublet Modules for the SIS100 Heavy Ion Synchrotron*, IEEE Transactions on Applied Superconductivity, vol. 26, no. 3, pp. 1–4 (2016), DOI: [10.1109/TASC.2016.2540165](https://doi.org/10.1109/TASC.2016.2540165).
- [7] Roux C. *et al.*, *The optimised sc dipole of SIS100 for series production*, IOP Conf. Ser.: Mater. Sci. Eng., vol. 171, no. 1, p. 012108 (2017), DOI: [10.1088/1757-899X/171/1/012108](https://doi.org/10.1088/1757-899X/171/1/012108).



- [8] Kovalenko A. et al., *The FAIR SIS100 Synchrotron: Engineering Design of Superconducting Magnetic Modules*, IEEE Transactions on Applied Superconductivity, vol. 20, no. 3, pp. 180–183 (2010), DOI: [10.1109/TASC.2010.2042441](https://doi.org/10.1109/TASC.2010.2042441).
- [9] Michna M., Wilk A., Ziółko M., Wołoszyk M., Swędrowski L., Szwangruber P., *Detection of inter-turn faults in transformer winding using the capacitor discharge method*, Open Physics, vol. 15, no. 1, pp. 979–983 (2017), DOI: [10.1515/phys-2017-0121](https://doi.org/10.1515/phys-2017-0121).
- [10] Wołoszyk M. et al., *Condition monitoring of superconducting magnets*, First World Congress on Condition Monitoring-WCCM 2017, London (2017).
- [11] Wołoszyk M., Ziółko M., Swędrowski L., *Diagnostyka obwodów elektrycznych magnesów nadprzewodzących*, Zeszyty Naukowe Wydziału Elektrotechniki i Automatyki Politechniki Gdańskiej, vol. 50, pp. 103–107 (2016).
- [12] Świsulski D., Wołoszyk M., Wołoszyn M., Ziółko M., Rafiński L., Stafiniak A., *Testing of the Superconducting Magnets Frequency Characteristics*, Elektronika ir Elektrotechnika, vol. 103, no. 7, pp. 39–42 (2015), DOI: [10.5755/j01.eee.103.7.9272](https://doi.org/10.5755/j01.eee.103.7.9272).
- [13] Mierau A. et al., *Testing of Series Superconducting Dipole Magnets for the SIS100 Synchrotron*, IEEE Transactions on Applied Superconductivity, vol. 29, no. 5, pp. 1–7 (2019), DOI: [10.1109/TASC.2019.2904693](https://doi.org/10.1109/TASC.2019.2904693).
- [14] Walter W. et al., *SIS100 Dipole Manufacturing: Experience From the First of Series*, IEEE Transactions on Applied Superconductivity, vol. 24, no. 3, pp. 1–4 (2014), DOI: [10.1109/TASC.2013.2285832](https://doi.org/10.1109/TASC.2013.2285832).
- [15] Fischer E., Khodzhbagiyani H.G., Kovalenko A.D., *Full Size Model Magnets for the FAIR SIS100 Synchrotron*, IEEE Transactions on Applied Superconductivity, vol. 18, no. 2, pp. 260–263 (2008), DOI: [10.1109/TASC.2008.922261](https://doi.org/10.1109/TASC.2008.922261).
- [16] Iwasa Y., Leupold M., Weggel R., Hale J., Williams J., *Diagnosis and analysis of an electrical short in a superconducting magnet*, IEEE Transactions on Magnetics, vol. 19, no. 3, pp. 704–706 (1983), DOI: [10.1109/TMAG.1983.1062404](https://doi.org/10.1109/TMAG.1983.1062404).
- [17] Takeuchi K., Asano K., Hayashi H., *A diagnosis method for properties of superconducting magnet using fast current discharge*, IEEE Transactions on Applied Superconductivity, vol. 11, no. 1, pp. 2595–2598 (2001), DOI: [10.1109/77.920399](https://doi.org/10.1109/77.920399).
- [18] Stafiniak A., Szwangruber P., Freisleben W., Floch E., *Electrical Integrity and its Protection for Reliable Operation of Superconducting Machines*, Phys. Procedia, vol. 67, pp. 1106–1111 (2015), DOI: [10.1016/j.phpro.2015.06.171](https://doi.org/10.1016/j.phpro.2015.06.171).
- [19] Grubic S., Restrepo J., Aller J., Lu B., Habetler T., *A New Concept for Online Surge Testing for the Detection of Winding Insulation Deterioration in Low-Voltage Induction Machines*, Transactions on Industry Applications, IEEE, vol. 47, pp. 2051–2058 (2011), DOI: [10.1109/TIA.2011.2161972](https://doi.org/10.1109/TIA.2011.2161972).
- [20] Marquardt D.W., *An Algorithm for Least-Squares Estimation of Nonlinear Parameters*, Journal of the Society for Industrial and Applied Mathematics, vol. 11, no. 2, pp. 431–441 (1963), DOI: [10.1137/0111030](https://doi.org/10.1137/0111030).
- [21] LabVIEW, <https://www.ni.com/pl-pl/shop/labview.html>, accessed January 2022.
- [22] 2022National Instruments, <https://www.ni.com/pl-pl.html>, accessed January 2022.
- [23] GSI Helmholtzzentrum für Schwerionenforschung, [https://www.gsi.de/en/about\\_us](https://www.gsi.de/en/about_us), accessed January 2022.